https://doi.org/10.55415/deep-2023-0039.v2

STING agonist delivery by lipid calcium phosphate nanoparticles enhances immune activation for neuroblastoma

Feng Bo[a,b], Xiao Lu[a], Guangqin Zhang[b], Libo Zhao[a],Mei Dong [a,*]

[a]Clinical Research Center, Beijing Children's Hospital, Capital Medical University, National Center for Children's Health, Beijing, 100045, People's Republic of China

[b]School of Basic Medicine and Clinical Pharmacy, China Pharmaceutical University, Nanjing, 211198, People's Republic of China

Correspondence: Mei Dong, Clinical Research Center, Beijing Children's Hospital, Capital Medical University, National Center for Children's Health, Beijing, People's Republic of China, Tel +86-010-59616370, Email meidong11290926@126.com

https://doi.org/10.55415/deep-2023-0039.v2

Abstract

Neuroblastoma (NB) is a common solid tumor in children and infants, with its formation and regression closely linked to the tumor-host immune mechanism. STING agonists, particularly cyclic dinucleotide (CDN), have promising potential in NB therapy by generating innate and adaptive immune stimulation, leading to tumor control. In vivo CDN delivery is challenging due to its negative charge, hydrophilicity, and susceptibility to degradation by phosphodiesterase, hindering its effectiveness. Thus, our study proposed four methods to load CDN into liposomes, using 2',3'-cGAMP as the model drug. Lipid nanoparticles were prepared, followed by physicochemical characterization. Subsequently, cellular inhibition and immune stimulation were investigated. As a result, lipid calcium phosphate nanoparticles (LCP-NP) possessed the highest encapsulation efficiency among the four preparation methods, with a diameter of 82.57 ± 3.72nm. LCP-NP maintained size stability under refrigeration conditions at 4℃ within 48 hours. The surface of the liposome was positively charged. Compared with free cGAMP, LCP-NP resulted in a slower release, enhanced cytotoxicity against tumor cells, greater activation of the cGAS-STING pathway, and increased expression of the immune factors. These findings clearly demonstrated the effectiveness of the liposomal delivery system for cGAMP and provided a promising strategy for the treatment of NB.

Keywords: lipid calcium phosphate nanoparticles, 2',3'-cGAMP, STING agonists, neuroblastoma, immunity therapy

https://doi.org/10.55415/deep-2023-0039.v2

1. Introduction

Neuroblastoma (NB) is one of the most common extracranial solid tumors in children and infants. It occurs in approximately 25-50 cases per million and accounts for 10% to 20% of pediatric malignancy deaths [1]. High risk NB (HRNB) is diagnosed when MYCN amplification is greater than stage 1 or age ≥ 18 months with stage 4 disease. Roughly 50% of NB cases are classified as HRNB. [2]. MYCN gene is a critical regulator of cell growth and proliferation. Amplification of MYCN is a common genetic alteration in neuroblastoma that is associated with poor prognosis, advanced disease stage, aggressive tumor behavior, and poor patient outcomes [3].

Treatment of NB involves three phases: induction, consolidation, and maintenance therapy. Options include chemotherapy, surgery, high-dose chemotherapy with autologous stem cell rescue, radiotherapy, and immunotherapy [4]. Low and intermediate-risk patients have a 5-year survival rate of approximately 90% to 85% [5]. However, high-risk patients have a significantly lower 5-year survival rate, averaging 50% [6]. Most HRNB patients relapse and die of drug-resistant disease, despite initial chemotherapy [7]. New treatment options are urgently needed for HRNB.

Various immunotherapies have shown promise for treating NB, but T-cell infiltration in the TME remains a challenge for effective treatment [8]. Although immune checkpoint blocking (ICB) antibodies targeting PD-L1 have shown efficacy for low and intermediate-risk NB, its effectiveness is limited for high-risk cases due to the lack of T-cell infiltration in the tumor microenvironment [9]. Monoclonal antibodies (mAb) therapy -targeting disialoganglioside (GD2) overexpressed on NB cells has been shown to improve the prognosis of NB patients [10].

https://doi.org/10.55415/deep-2023-0039.v2

However, despite this improvement, the 5-year survival rate for HRNB remains less than 50% [11]. New immunotherapy approaches are being researched to address these challenges.

STING agonists have raised wide attention in the immunotherapy of NB. STING agonists possess an appealing property in that their response is not dependent on T cells within the tumor microenvironment. [5]. Microbial-released DNA or DNA shed by dying tumor cells, or STING agonists are sensed by intracellular DNA sensors such as cyclic GMP-AMP synthase (cGAS), leading to activation of the STING signaling pathway in dendritic cells [6]. This results in their phenotypic maturation. After activation, downstream signaling pathways such as IRF3 and NF-κB are activated, resulting in the production of type I interferons and other cytokines, such as CXCL10, which activate CD8 T cells through a cascade of events [7]. STING agonists can stimulate antigen presentation by activating dendritic cells and promote T cell activation as well [6]. Previous studies have shown that STING agonists could be used in NB immunotherapy. Research by Lihong Wang-Bishop et al. indicated that STING-NPs incorporating PEG-DBP copolymer were effective in inhibiting the growth of mouse neuroblastoma, extending survival, and inducing immune memory to prevent tumor recurrence [12]. As a result, STING agonists exhibit great promise for the treatment of NB.

However, the main challenge of STING agonists' application lies in the *in vivo* delivery. For instance, cyclic dinucleotide (CDN) is a negatively charged hydrophilic small molecule, which limits its entry into the cytoplasm. It is easily degraded and inactivated by ectonucleotide pyrophosphatase/phosphodiesterase, which seriously affects its efficacy. To solve these problems, researchers designed various CDN delivery systems based on biomaterials, such as cationic silica nanoparticles for local drug delivery [13], poly (β-amino ester) polymer

nanoparticles [14], etc. However, the clinical application of polymer nanoparticles is limited due to multiple disadvantages, such as complex design and synthesis process, side effects induced by the added organic solvent, and insufficient biocompatibility [15].

As a comparison, liposomes can effectively entrap water-soluble molecules, improve drug stability and reduce drug toxicity. Moreover, the industrial production technology for liposomes is much more mature, and various liposomal drug delivery systems have been approved for clinical use now [16]. For example, liposome-encapsulated doxorubicin hydrochloride (Doxil) was approved for marketing by the US Food and Drug Administration (FDA) for the first time in 1995, and its safety has been extensively verified [17].

Thus, this paper developed a liposome delivery system for an active natural STING agonist, 2',3'-cGAMP, to improve cellular delivery efficiency. Specifically, we prepared liposomes loaded with 2',3'-cGAMP by four methods: thin-film dispersion method, ammonium sulfate gradient method, calcium acetate gradient method, and lipid calcium phosphate nanoparticle method. Among these four methods, lipid calcium phosphate nanoparticles (LCP-NP) achieved the highest encapsulation efficiency. Hence, more detailed physicochemical characterization and in-vitro experiments were conducted on LCP-NP. LCP-NP can maintain a stable particle size at 4℃ for 48 hours. Its surface was positively charged. Compared with free cGAMP, LCP-NP resulted in a slower release, enhanced cytotoxicity against tumor cells, greater activation of the cGAS-STING pathway, and increased expression of immune factors such as CXCL9, TNF-α, and IFN-β. This study provided a perspective on the delivery of STING agonists.

2. Materials and Methods

2.1 Materials

In this study, 2',3'-cGAMP was purchased from MedChemExpress (Shanghai, China). Igepal was purchased from Shanghai Macklin Biochemical Co., Ltd.(Shanghai, China). 1,2-dioleoyl-3-trimethylammoniumpropane, monochloride(DOTAP) was purchased from Shanghai kanglang Biotechnology Co., Ltd.(Shanghai, China). 1,2-distearoyl-sn-glycero-3-phosphoethanolamine-N-[methoxy (polyethylene glycol)-2000](DSPE-PEG2000) was purchased from A.V.T. Pharmaceutical Co.,Ltd.(Shanghai, China). Na_2HPO_4, $(NH_4)_2SO_4$, $CaCL_2$, egg phosphatidylcholine (EPC), cholesterol, and the Cell Counting Kit-8 (CCK8) were obtained from Solarbio Technology Co., Ltd (Beijing, China). TRIeasy™ Total RNA Extraction Reagent, Hifair® III 1st Strand cDNA Synthesis SuperMix for qPCR, Hieff UNICON® Universal Blue qPCR SYBR Green Master Mix were obtained from Yeasen Biotechnology Co., Ltd. (Shanghai, China). Fetal bovine serum (FBS) was supplied by PAN-Biotech GmbH (Adenbach, Germany). QUANTI-Blue™ Solution was purchased from InvivoGen (California, America).

2.2 Preparation of cGAMP liposomes by four different methods

2.2.1 Thin-film dispersion method. The ingredients of the recipe were precisely weighed and added to an eggplant-shaped bottle, followed by the addition of an appropriate amount of chloroform to ensure full dissolution. The solvent was then removed via rotary evaporation under reduced pressure at a 40℃ water bath to produce a homogeneous film. Next, 330 μl of the aqueous cGAMP solution was added and the mixture was vigorously vortexed. The drug was loaded in a water bath at 70℃ for 1 h. Ultrasonication was carried out for 4 minutes until a light blue emulsion appeared. The obtained nanoparticles were abbreviated as TFD-NP.

2.2.2 Ammonium sulfate gradient method. Materials in the recipe were weighed precisely and placed into an eggplant-shaped bottle. Chloroform was added to dissolve the materials, and

https://doi.org/10.55415/deep-2023-0039.v2

the solvent was evaporated under reduced pressure in a 40℃ water bath to form a uniform film. The film was hydrated with 1 mL of 120 mmol/L aqueous ammonium sulfate solution, followed by vortexing and ultrasound treatment until it showed light blue opalescence. After cooling to room temperature, free ammonium sulfate was removed by the Sephadex G-50 gel column to obtain blank liposomes. The liposomes were then mixed with 330ul cGAMP aqueous solution and loaded in a water bath at 70℃ for 1 hour. After the solution was cooled to room temperature, the free cGAMP was removed by a Sephadex G-50 gel column to obtain cGAMP-liposomes. The obtained nanoparticles were referred to as ASG-NP.

2.2.3 Calcium acetate gradient method. Each ingredient in the recipe was accurately weighed and added to an eggplant-shaped bottle. Chloroform was added to achieve full dissolution, and the resulting solution was evaporated under reduced pressure in a 40℃ water bath to form a uniform film. Next, a 130mmol/L calcium acetate aqueous solution (adjusted to pH = 6 with glacial acetic acid) was added, followed by vortexing and hydration at 70℃ for 15 minutes. The mixture was ultrasonicated for 4 minutes until it appeared as a light blue opalescence. Free calcium acetate was removed using a Sephadex G-50 gel column to obtain blank liposomes, which were then mixed with 330ul of cGAMP aqueous solution. The drug was loaded in a water bath at 70℃ for 1 hour. After the solution was cooled to room temperature, the free cGAMP was removed by a Sephadex G-50 gel column to obtain cGAMP-liposomes. The nanoparticles are abbreviated as CAG-NP.

2.2.4 Lipid calcium phosphate nanoparticle method. 300 μL of Na_2HPO_4 was meticulously added to a mixture of 15mL of cyclohexane/Igepal (71:29), followed by the addition of 200 μL of DOPA. The resulting mixture was sonicated to obtain the Na_2HPO_4 phase microemulsion.

https://doi.org/10.55415/deep-2023-0039.v2

Similarly, 300 μL of $CaCl_2$ containing cGAMP was added to 15mL of cyclohexane/Igepal (71:29) mixture and sonicated. After the ultrasound, the $CaCl_2$ phase microemulsion was obtained. The two-phase microemulsion was thoroughly mixed for 20 minutes. To break the demulsification, 30 mL of absolute ethanol was added. The mixture was then centrifuged at 16,000 g for 20 minutes and washed 2-3 times with ethanol. The resulting CaP pellets were dissolved in 1 mL of chloroform for later use. The ingredients in the recipe were meticulously weighed and mixed with the CaP-core, then the chloroform was evaporated at 40℃. Tris-HCL buffer was added, followed by ultrasonication for 4 minutes to obtain cGAMP-liposomes, which were named LCP-NP [18-20]. The formulations for all four methods are presented in **Table 1**.

Table 1 Preparation recipes for different methods.

Formulation	DOTAP(mg)	EPC(mg)	cholesterol(mg)	DSPE-PEG2000(mg)
TFD-NP	16.9		3	1.07
ASG-NP		16.9	3	1.07
CAG-NP		16.9	3	1.07
LCP-NP	3.72		1.93	4.2

2.3 Particle size and zeta potential analysis

The prepared liposomes were subjected to dynamic light scattering (DLS) analysis. Particle size and polydispersity were determined using an NKT-N9 nanoparticle size analyzer. The wavelength of the laser beam of the NKT-N9 was set at 633 nm. The refractive index was 1.33. The polydispersity indicated the uniformity of particle size, and the smaller the polydispersity, the more uniform the particles were. Zeta potential was determined using the Malvern Zetasizer Nano ZS instrument. The wavelength of the laser beam of the instrument was set at 633 nm. The angle between the incident beam and the scattered beam was 90°. Each sample was measured for 15 cycle times, and the measurement temperature was set at 25℃.

https://doi.org/10.55415/deep-2023-0039.v2

2.4 Determination of liposomes encapsulation efficiency

The content of the drug was determined by high-performance liquid chromatography (HPLC). Accurately aspirate the liposomes. The liposomes were destroyed by adding 1% Triton X-100 solution and depolymerized by vortexing to release the encapsulated cGAMP. The content of cGAMP was determined using reverse-phase HPLC. The following chromatographic conditions were employed in the analysis: Agilent ZORBAX SB-C18 (4.6 × 250 mm, 5 μm) column with a detection wavelength of 260 nm. Mobile phase: Phase A 50mM TEAA pH=7.2, Phase B ACN. The column temperature was set at 30℃. The gradient elution process was as follows[21, 22]:

Time/min	0	20	23	25	35
A Mobile phase	100	87	60	100	100
B Mobile phase	0	13	40	0	0

2.5 Praticles size stability of liposomes

The prepared liposomes were placed at 4℃ for observation and photography within 48 hours after preparation. The stability of the liposomes was investigated by measuring the particle size and polydispersity coefficient of the liposomes.

2.6 Microscopy characterization and *in vitro* release of LCP-NP

The surface morphology of LCP-NPs was characterized through transmission electron microscopy (TEM, JOEL, JEM 2100). It occurred after negative staining via a 1% uranyl acetate solution at an accelerating voltage of 80 kV.

For *in vitro* release experiment, free cGAMP or LCP-NP were added to activated dialysis bags (MWCO3500). These bags were then placed into a conical flask containing the appropriate amount of release medium and shaken at a constant temperature of 37℃ and 100 rpm/min

using an oscillator. At specific time points (0.5, 1, 2, 3, 4, 5, 6, 8, 10, 24h), a volume of 150 μL of the release solution was collected. Fresh release medium (150 μL) was added to the conical flask after each sampling and the mixture was continued to shake. After 24 hours, the dialysis clips clamped at both ends of the dialysis bag were loosened, and a sample was taken after stirring for another half an hour. The cGAMP content was determined using reverse-phase HPLC and the cumulative drug release rate was calculated.

2.7 CCK8 assay of LCP-NP

Neuroblastoma neuro-2a cells were seeded at a density of 1×10^5 cells/mL in a 96-well plate, with 100 μL per well. To maintain a humid environment, 200 μL of PBS was added to the surrounding wells. Neuro-2a cells were placed in an incubator and cultured overnight. The culture medium was aspirated, and 200 μL of drug-containing serum-free medium was added to each well. The plate was then incubated for 8 hours with different concentrations of the drug (0.5/1/5/10/50/100 μM). After removing the medium, 100 μL of the serum-free medium was added to each well, followed by 10 μL of CCK8 solution. The plate was incubated for 1 hour in the incubator, and the absorbance at 450 nm was measured using a microplate reader. Cell viability and IC50 were calculated based on the results.

2.8 Evaluation of cGAS-STING pathway activation in reporter cells

RAW blue ISG cells were seeded in a 96-well plate. A series of drug concentration gradients were set to 0.1/0.5/1/3/10/30 μM. After adherence, the cells were incubated with LCP-NP and free cGAMP for 2 hours. After the incubation, the drug was discarded and replaced with a serum-containing medium for 22 hours to generate secreted embryonic alkaline phosphatase (SEAP). To assess SEAP (secreted alkaline phosphatase) activity, 50 μL of cell supernatant from

each well was transferred into a new 96-well plate. Then, 150 μL of QUANTI-Blue™ Solution was added to each well, followed by incubation at 37°C in an incubator. After color development, the absorbance of the supernatant at 620 nm was measured using a microplate reader. [23].

2.9 Gene expression analysis

RT-qPCR was used to determine the expression of the immune factors in DC2.4 cells treated with different preparations [6]. DC2.4 cells were homogeneously seeded in six-well plates and incubated overnight. The LCP-NP and free cGAMP were diluted to 1 μg/mL in serum-free medium and the cells were treated for 6 hours. According to the TRIeasy™ Total RNA Extraction Reagent instructions, cellular mRNA was extracted. The RNA concentration was determined using NanoDrop2000. The reverse transcription was carried out to synthesize cDNA using Hifair® III 1st Strand cDNA Synthesis SuperMix for qPCR according to the manufacturer's instructions. Real-Time Quantitative PCR(RT-qPCR) was performed by ABI 7500 Real-Time PCR. GAPDH was used as an internal reference. The relative expression changes were calculated by the ΔΔCt method [24, 25]. The primer sequences were as follows:

mmu-Gapdh-F	AGGTCGGTGTGAACGGATTTG
mmu--Gapdh-R	TGTAGACCATGTAGTTGAGGTCA
mmu-CXCL9-F	GGAGTTCGAGGAACCCTAGTG
mmu-CXCL9-R	GGGATTTGTAGTGGATCGTGC
mmu-TNF-α-F	CCCTCACACTCAGATCATCTTCT
mmu-TNF-α-R	GCTACGACGTGGGCTACAG
mmu-IFN-β-F	CAGCTCCAAGAAAGGACGAAC
mmu-IFN-β-R	GGCAGTGTAACTCTTCTGCAT

2.10 Statistical analysis

All data subjected to statistical analysis were obtained from at least three parallel experiments. Multiple groups were analyzed using GraphPad software. A p-value ≤ 0.05 was

considered statistically significant.

3. Results and discussion

3.1 Characterization of physicochemical properties of four liposomes

The high hydrophilicity of cGAMP presents challenges when formulating it into liposomes, such as suboptimal drug encapsulation efficiency and variable drug release kinetics[26]. In addition, the size and distribution of liposomes can be influenced by the preparation method. To address these challenges, we evaluated four different methods for formulating cGAMP-loaded liposomes, with the goal of identifying the optimal method for achieving high drug encapsulation efficiency. The methods tested include the thin-film dispersion method, ammonium sulfate gradient method, calcium acetate gradient method, and lipid calcium phosphate nanoparticle method, with corresponding obtained nanoparticles, abbreviated as TFD-NP, ASG-NP, CAG-NP, and LCP-NP, respectively. As seen in **Figure 1,** the appearance of liposomes prepared by these four methods was translucent and slightly blue-opalescent.

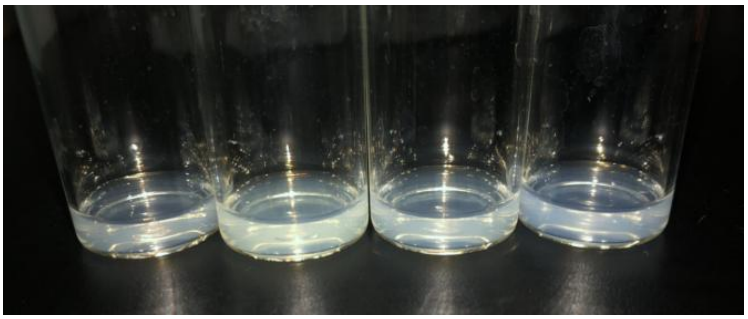

Figure 1 Appearance of liposomes prepared by four methods (left to right): TFD-NP, ASG-NP, CAG-NP, LCP-NP.

The particle size and zeta potential analysis are shown in **Table 2** and **Figure 2**. The particle size of TFD-NP and LCP-NP was between 80 and 100 nm. The particle size of ASG-NP, and CAG-NP were between 100 and 120 nm with a dispersibility below 0.200 and good preparation

https://doi.org/10.55415/deep-2023-0039.v2

reproducibility. The Zeta potential of ASG-NP and CAG-NP were negative, which might go against the cellular uptake, due to the electrostatic repulsion to the cell membrane.

Table 2 Particle size, zeta potential, and encapsulation efficiency analysis.

Nanoparticle	Size (nm)	PDI	Zeta (mv)	Encapsulation efficiency (%)
TFD-NP	85.54 ± 3.86	0.139 ± 0.02	58.1 ± 17.3	13.63 ± 1.02
ASG-NP	119.07 ± 5.34	0.060 ± 0.01	-19.7 ± 6.8	5.84 ± 0.78
CAG-NP	102.35 ± 4.62	0.071 ± 0.01	-24.7 ± 11.6	9.15 ± 0.92
LCP-NP	82.57 ± 3.72	0.157 ± 0.03	15.9 ± 4.3	21.24 ± 1.28

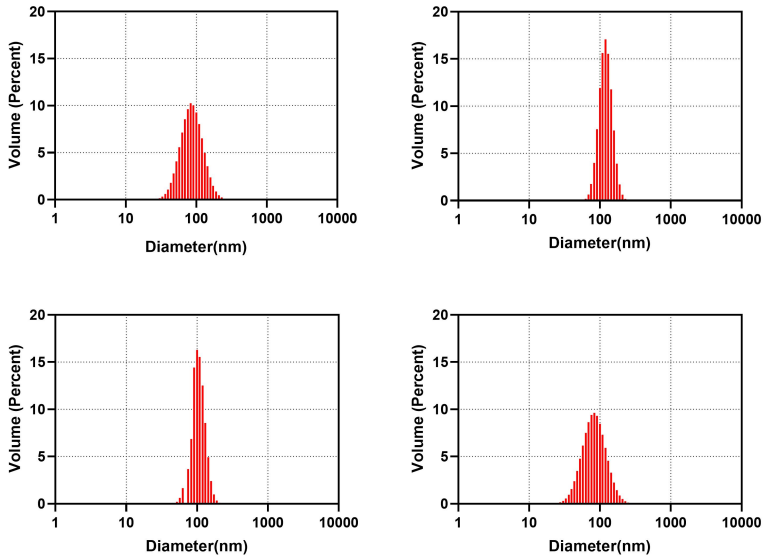

Figure 2 Particle size distribution of STING agonist-loaded liposomes. (A) TFD-NP. (B) ASG-NP. (C) CAG-NP. (D) LCP-NP.

Liposome encapsulation efficiencies are listed in **Table 2**. Water-soluble small molecules, such as 2',3'-cGAMP (solubility of 50 mg/ml), generally exhibit a lower encapsulation efficiency as they tend to leak out of the liposomes due to their high solubility in water [27]. LCP-NP had the highest encapsulation among the four methods. As shown in **Figure 3,** a pH-sensitive calcium phosphate (CaP) core was prepared by the lipid calcium phosphate nanoparticle method. In this study, stable CaP cores were prepared using a water/oil microemulsion. The CaP cores were coated with an inner layer of DOPA and an outer layer of cationic lipids, DOTAP,

https://doi.org/10.55415/deep-2023-0039.v2

cholesterol, and DSPE-PEG, forming a hollow spherical structure with a lipid bilayer. The hollow structure of the CaP core, which was formed in water droplets, could provide an opportunity to capture water-soluble drugs, at least in part. The lipid coating prevented the CaP core from aggregating during the centrifuge separation step and made it soluble in chloroform. After

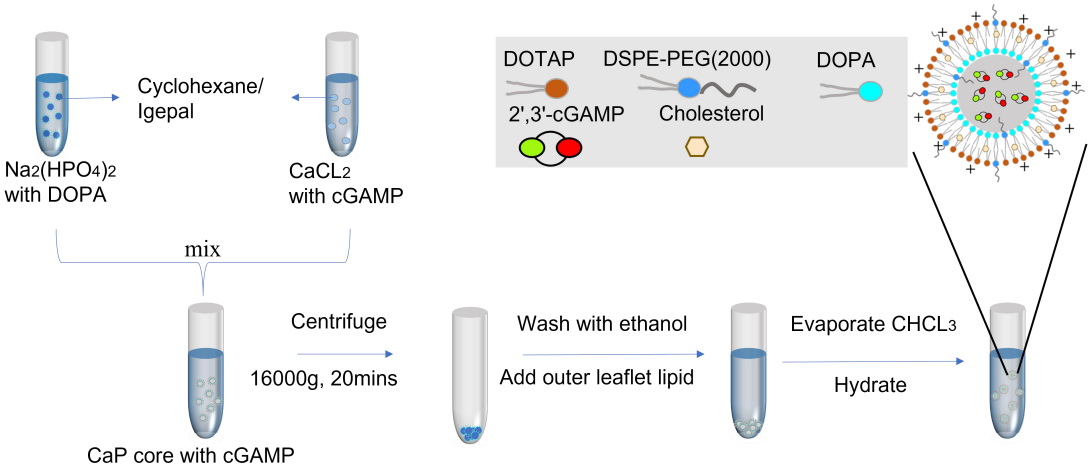

adding the outer lipid layer, the chloroform was evaporated, and finally, the lipid bilayer was self-assembled in an aqueous solution.

Figure 3 Preparation outline for LCP-NP and corresponding lipid bilayer structure. CaP-core with GAMP was obtained, followed by lipid addition to prepare LCP-NP. LCP-NP: lipid calcium phosphate nanoparticles.

It has been reported that this method has been used for the encapsulation of nucleic acid drugs *in vivo*. cGAMP is a small molecule of cyclodinucleic acid class. This experiment demonstrated the feasibility of LCP-NP for the encapsulation of cGAMP.

Next, we investigated the particle size stability of liposomes at different time points after formulation. The results are shown in **Figure 4**. Under the storage conditions of 4°C for 48 hours, the appearance of the solution remained unchanged, appearing as a clear, milky blue solution and the particle size of the liposomes remained stable. Predictably liposomes could keep stable during the subsequent cell experiments in which drug treatments were carried out

https://doi.org/10.55415/deep-2023-0039.v2

within 48 h.

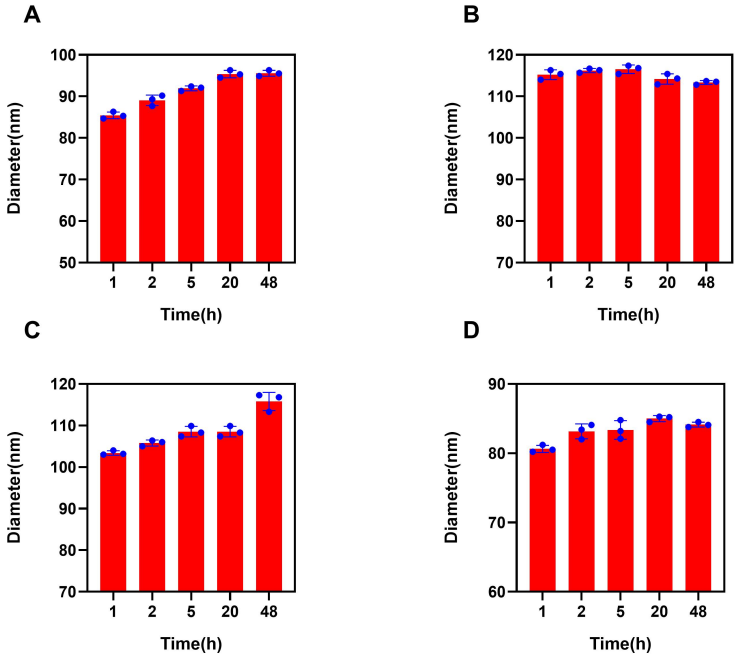

Figure 4 Particle size stability of STING agonist-loaded liposomes under refrigeration (4℃) for 48 hours. (A) TFD-NP. (B) ASG-NP. (C) CAG-NP. (D) LCP-NP.

3.2 Microscopy characterization and *in vitro* release of LCP-NP

Given that LCP-NP had good physicochemical properties, and the encapsulation efficiency of LCP-NP was the highest among the four liposomes. Subsequently, LCP-NPs were selected for detailed morphological and *in vitro* release studies. The electron microscope picture is shown by TEM in **Figure 5A**. It showed that LCP-NP nanoparticles were spherical, and the particle size results were similar to those determined by DLS. The *in vitro* release curve is shown in **Figure 5B**. The free cGAMP solution released about 70% within 0.5 h, whereas LCP-NP released about 50%. In contrast, LCP-NP had a certain sustained-release effect. Within 24 hours, the cumulative release of LCP-NP was within 80%.

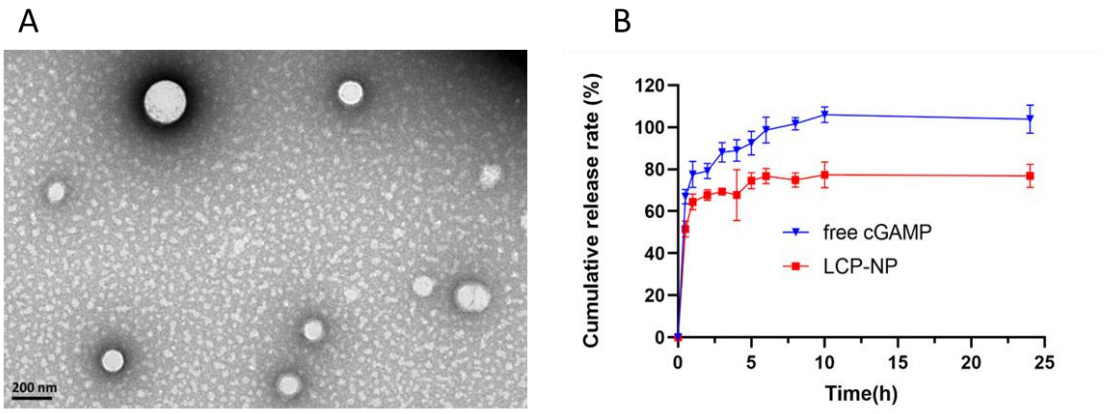

Figure 5 (A) Transmission electron microscopy image. (B) The release profile of cGAMP from free cGAMP or LCP-NP. The preparations were added to dialysis bags and released in PBS at 37℃. The cGAMP content in the release medium was periodically measured by HPLC.

3.3 Cytotoxicity of LCP-NP

Given the previous literature reports, it has been documented that STING agonists exhibit immunomodulatory effects at low concentrations, while at high concentrations, they could induce tumor cell death[28]. Our objective was to comprehensively investigate the immunomodulatory properties of LCP-NP and its potential for inhibiting cell growth. Therefore, we examined the formulation's inhibitory effects on neuro-2a cell growth at various concentrations. Our experimental findings showed a dose-dependent inhibitory effect of the free cGAMP and LCP-NP on neuro-2a cell growth, speculating a degree of tumor cell growth inhibition. The IC50 of the LCP-NP was 2.16 μM, and the IC50 of the free cGAMP solution was 16.98 μM. Calcium phosphate and DOTAP has been generally recognized as safe [29, 30]. We speculated that the increased cytotoxicity of LCP-NP on neuro-2a cells compared to free cGAMP was due to increased cellular uptake of cGAMP, and likely resulted from the electrostatic interactions on the surface of LCP-NP[31]. According to WANG-BISHOP L's report, STING agonists could directly activate caspase-3 in neuro-2a cells and induce tumor cell death[4]. Additionally, Sokolowska, O's study highlighted the complexity of the STING pathway

in cancer cells, as the response of tumor cells to STING activation might exhibit inhibitory or growth-promoting effects[32]. There is currently no consensus on whether STING activation in cancer cells leads to cell death, necessitating further study to determine the impact of STING activation on cancer cell viability.

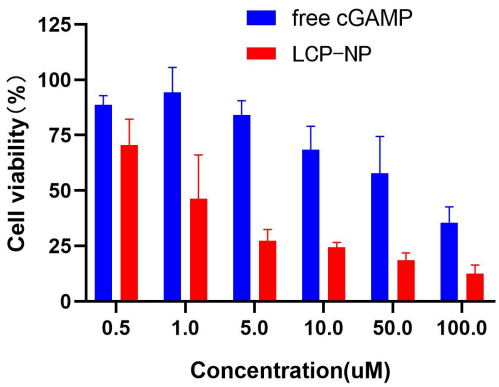

Figure 6 Cytotoxic effect of LCP-NP on neuro-2a cells. Growth inhibition was assessed using a CCK8 assay after 8 hours of incubation. Each value represents as the mean ± SD (n = 6).

3.4 cGAS-STING pathway activation by LCP-NPs

To explore the effect of formulations in stimulating type I interferon production, RAW-Blue ISG cells were employed to investigate the impact of LCP-NP on the cGAS-STING pathway, as macrophages played a crucial role in cGAMP-mediated antitumor activity in the tumor microenvironment and secrete reporter SEAP upon stimulation of the cGAS-STING pathway by cGAMP. SEAP is capable of reacting with QUANTI-Blue™ Solution to indicate the level of cGAS-STING pathway activation through a colorimetric assay, where a higher absorbance corresponds to an increased production of SEAP and a stronger activation of the cGAS-STING pathway. **Figure 7** illustrates the dose-dependent effect of LCP-NP on cGAS-STING pathway activation in RAW-Blue ISG. The results showed that LCP-NP can effectively activate the cGAS-STING pathway in RAW-Blue ISG cells in a dose-dependent manner. The increasing concentrations of

https://doi.org/10.55415/deep-2023-0039.v2

LCP-NP led to a stronger activation of the cGAS-STING pathway. The inability of free cGAMP to activate the cGAS-STING pathway may be due to its limited cellular uptake. While LCP-NP, possessing a positively charged surface, can readily penetrate into cells and trigger cGAS-STING pathway activation as **Scheme 1** [18, 31].

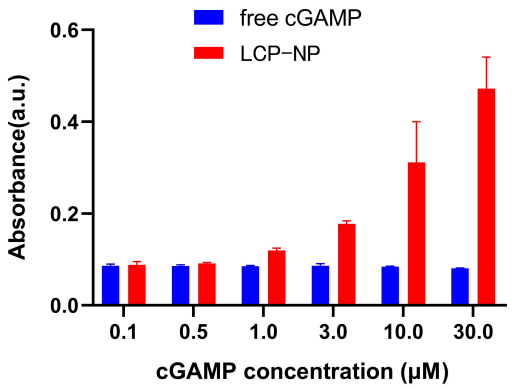

Figure 7 Dose-response curves of cGAMP preparations on RAW-Blue ISG cells. Reporter enzyme production was measured in response to cGAMP stimulation, indicating activation of the cGAS-STING pathway. Each value represents the mean ± SD (n = 3).

3.5 Immune factors expression

Previously, it has been reported that cGAMP can activate the cGAS-STING pathway of APC, resulting in increased expression of downstream immune factors. In this study, we measured mRNA expression levels of these immune factors to further demonstrate the activation of the cGAS-STING pathway by LCP-NP. After incubation of LCP-NP and free drug with antigen-presenting cells DC2.4 respectively, immune factor expression levels were assessed by RT-qPCR. The results are showed in **Figure 8**. Compared to free cGAMP, LCP-NP was found to significantly upregulate the expression of several immune factors, such as CXCL9, TNF-α, and IFN-β. Specifically, LCP-NP resulted in an 8-fold increase in CXCL9 expression, a 77-fold increase in TNF-α expression, and a 5-fold increase in IFN-β expression. CXCL9 is the key to recruiting effector T cells into tumors. Tumor necrosis factor TNF-α is a cytokine that induces rapid

https://doi.org/10.55415/deep-2023-0039.v2

destruction of tumor blood vessels after STING agonist delivered to tumors [18, 24]. Type I interferon(IFN-β) is essential for the generation of antitumor T cell responses. As **Scheme 1** depicted, these findings suggested that LCP-NP could effectively deliver cGAMP into the cytoplasm of cells. After LCP-NPs enter the cells, the STING agonist released into the cytoplasm could enhance the activation of the cGAS-STING pathway in APC, causing APC to produce type I interferon and other cytokines, and finally activate CD8+T cells.

These results provided evidence for the potential use of LCP-NP as an immunotherapeutic agent for the treatment of cancers. Further studies are necessary to assess the effectiveness and safety of LCP-NP *in vivo*, as well as to explore the underlying mechanisms involved in the cGAS-STING pathway.

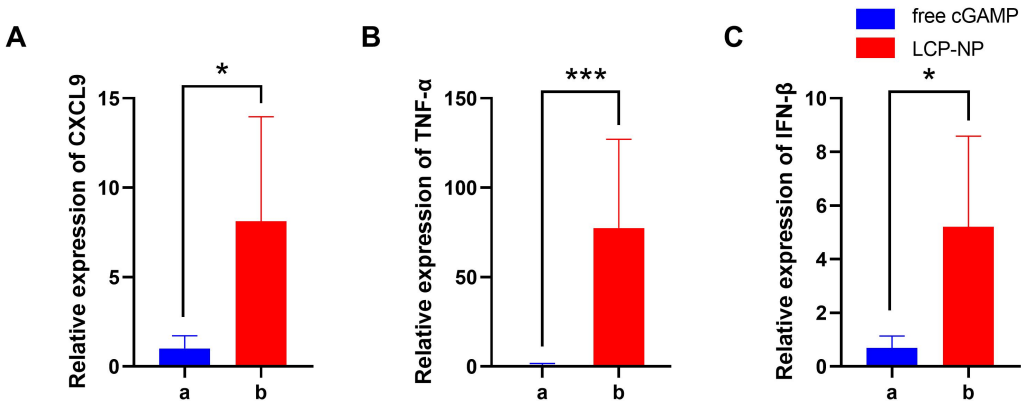

Figure 8 Gene expression levels in DC2.4 cells treated with free cGAMP or LCP-NP, respectively. Each value represents the mean ± SD (n = 3). *p<0.05, **p<0.01 and ***p<0.001.

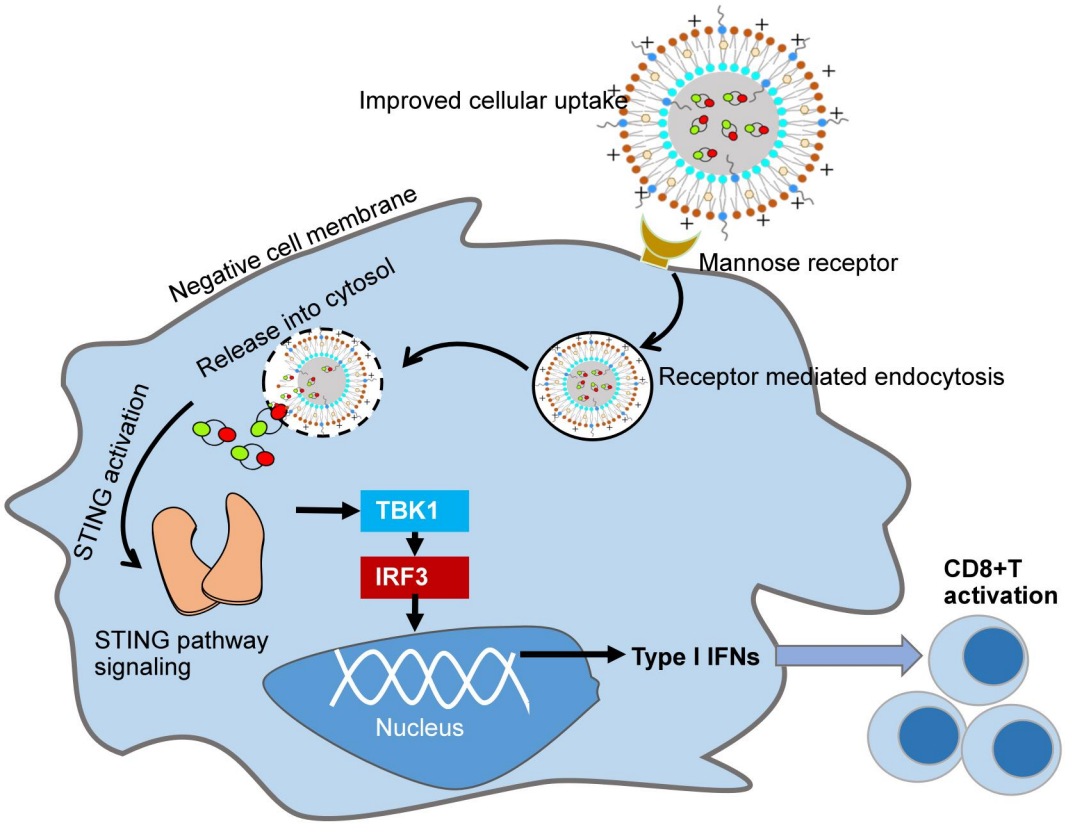

Scheme 1 The schematic diagram of LCP-NP entering antigen-presenting cells (APC)and enhancing immune stimulatory effects.

4. Conclusions

Liposomes are widely studied nanodrug carriers, which are biocompatible and biodegradable. It could effectively protect the encapsulated drugs from degradation and slowly release the drugs. In this study, cGAMP-loaded liposomes were prepared by four different methods. Lipid calcium phosphate nanoparticles with the highest encapsulation efficiency was selected to perform detailed physicochemical characterization and cellular experiments. The obtained LCP-NP exhibited ideal particle size and good stability. *In vitro* studies have demonstrated that LCP-NP increased cytotoxicity against neuro-2a cells, enhanced the activation of the cGAS-STING pathway, and upregulated the expression of immune factors. These findings indicated the potential of LCP-NP for the delivery of cGAMP. This system could provide a new prospect for NB immunotherapy. Its in-vivo effect is also worthy of further

exploration.

CRediT author statement

Bo Feng and Dong Mei designed and conducted the experiments, analyzed and interpreted the data, and participated in writing the manuscript. Dong Mei, Libo Zhao and Guangqin Zhang provided experimental materials and technical support, and contributed to experimental design and data analysis. Dong Mei and Xiao Lu were responsible for the overall project planning, design, experiment management, data analysis, and manuscript writing.

Declaration of competing interest

All authors have reviewed and approved the final version of the manuscript.

Acknowledgments

This work was sponsored by Beijing Natural Science Foundation, China (Grant L202048, L212013, 7232246), Beijing Nova Program, China (Grant Z201100006820009, 20220484219), and Beijing Hospitals Authority Youth Programme, (Grant QML20201201).

References

[1] Yang R, Zheng S, Dong R, Circulating tumor cells in neuroblastoma: Current status and future perspectives, Cancer Med.2022).

[2] Dubois S G, Macy M E, Henderson T O, High-Risk and Relapsed Neuroblastoma: Toward More Cures and Better Outcomes, Am Soc Clin Oncol Educ Book. 42(2022) 1-13.

[3] Otte J, Dyberg C, Pepich A, et al, MYCN Function in Neuroblastoma Development, Front Oncol. 10(2020) 624079.

[4] Wang-Bishop L, Wehbe M, Shae D, et al, Potent STING activation stimulates immunogenic cell death to enhance antitumor immunity in neuroblastoma, J Immunother Cancer. 8(2020).

[5] Lu X, Cheng H, Xu Q, et al, Encapsulation of STING Agonist cGAMP with Folic Acid-Conjugated Liposomes Significantly Enhances Antitumor Pharmacodynamic Effect, Cancer Biother Radiopharm.2021).

[6] Wang M, Sooreshjani M A, Mikek C, et al, Suramin potently inhibits cGAMP synthase, cGAS, in THP1 cells to modulate IFN-β levels, Future Medicinal Chemistry. 10(2018) 1301-1317.

[7] Wang-Bishop L, Wehbe M, Shae D, et al, Potent STING activation stimulates immunogenic cell death to enhance antitumor immunity in neuroblastoma, Journal for ImmunoTherapy of Cancer. 8(2019) e282.

[8] Layer J P, Kronmüller M T, Quast T, et al, Amplification of N-Myc is associated with a T-cell-poor microenvironment in metastatic neuroblastoma restraining interferon pathway activity

and chemokine expression, OncoImmunology. 6(2017).
[9] Srinivasan P, Wu X, Basu M, et al, PD-L1 checkpoint inhibition and anti-CTLA-4 whole tumor cell vaccination counter adaptive immune resistance: A mouse neuroblastoma model that mimics human disease, PLoS Med. 15(2018) e1002497.
[10] Sait S, Modak S, Anti-GD2 immunotherapy for neuroblastoma, Expert Rev Anticancer Ther. 17(2017) 889-904.
[11] Wienke J, Dierselhuis M P, Tytgat G, et al, The immune landscape of neuroblastoma: Challenges and opportunities for novel therapeutic strategies in pediatric oncology, Eur J Cancer. 144(2021) 123-150.
[12] Wang-Bishop L, Wehbe M, Shae D, et al, Potent STING activation stimulates immunogenic cell death to enhance antitumor immunity in neuroblastoma, J Immunother Cancer. 8(2020).
[13] An M, Yu C, Xi J, et al, Induction of necrotic cell death and activation of STING in the tumor microenvironment via cationic silica nanoparticles leading to enhanced antitumor immunity, Nanoscale. 10(2018) 9311-9319.
[14] Wilson D R, Sen R, Sunshine J C, et al, Biodegradable STING agonist nanoparticles for enhanced cancer immunotherapy, Nanomedicine. 14(2018) 237-246.
[15] Zhou Q, Zhou Y, Li T, et al, Nanoparticle-Mediated STING Agonist Delivery for Enhanced Cancer Immunotherapy, Macromol Biosci. 21(2021) e2100133.
[16] Sheng G T N D H, Advances in therapeutic nanodrug delivery systems for infectious lung diseases: a review, Acta Materia Medica. 1(2022).
[17] Barenholz Y, Doxil(R)--the first FDA-approved nano-drug: lessons learned, J Control Release. 160(2012) 117-134.
[18] Liu Y, Wang L, Song Q, et al, Intrapleural nano-immunotherapy promotes innate and adaptive immune responses to enhance anti-PD-L1 therapy for malignant pleural effusion, Nature Nanotechnology. 17(2022) 206-216.
[19] Liu Y, Crowe W N, Wang L, et al, An inhalable nanoparticulate STING agonist synergizes with radiotherapy to confer long-term control of lung metastases, Nature Communications. 10(2019).
[20] Li J, Yang Y, Huang L, Calcium phosphate nanoparticles with an asymmetric lipid bilayer coating for siRNA delivery to the tumor, Journal of Controlled Release. 158(2012) 108-114.
[21] Ablasser A, Goldeck M, Cavlar T, et al, cGAS produces a 2′-5′-linked cyclic dinucleotide second messenger that activates STING, Nature. 498(2013) 380-384.
[22] Gao J, Tao J, Liang W, et al, Identification and characterization of phosphodiesterases that specifically degrade 3'3'-cyclic GMP-AMP, Cell Res. 25(2015) 539-550.
[23] Koshy S T, Cheung A S, Gu L, et al, Liposomal Delivery Enhances Immune Activation by STING Agonists for Cancer Immunotherapy, Adv Biosyst. 1(2017).
[24] Chin E N, Yu C, Vartabedian V F, et al, Antitumor activity of a systemic STING-activating non-nucleotide cGAMP mimetic, Science. 369(2020) 993-999.
[25] Li S, Luo M, Wang Z, et al, Prolonged activation of innate immune pathways by a polyvalent STING agonist, Nature Biomedical Engineering. 5(2021) 455-466.
[26] Wehbe M, Wang-Bishop L, Becker K W, et al, Nanoparticle delivery improves the pharmacokinetic properties of cyclic dinucleotide STING agonists to open a therapeutic window for intravenous administration, Journal of Controlled Release. 330(2021) 1118-1129.
[27] Eloy J O, Claro D S M, Petrilli R, et al, Liposomes as carriers of hydrophilic small molecule

drugs: strategies to enhance encapsulation and delivery, Colloids Surf B Biointerfaces. 123(2014) 345-363.
[28] Chandra D, Quispe-Tintaya W, Jahangir A, et al, STING ligand c-di-GMP improves cancer vaccination against metastatic breast cancer, Cancer Immunol Res. 2(2014) 901-910.
[29] Sun M, Dang U J, Yuan Y, et al, Optimization of DOTAP/chol Cationic Lipid Nanoparticles for mRNA, pDNA, and Oligonucleotide Delivery, AAPS PharmSciTech. 23(2022) 135.
[30] Bisht S, Bhakta G, Mitra S, et al, pDNA loaded calcium phosphate nanoparticles: highly efficient non-viral vector for gene delivery, Int J Pharm. 288(2005) 157-168.
[31] Su T, Zhang Y, Valerie K, et al, STING activation in cancer immunotherapy, Theranostics. 9(2019) 7759-7771.
[32] Sokolowska O, Nowis D, STING Signaling in Cancer Cells: Important or Not? Arch Immunol Ther Exp (Warsz). 66(2018) 125-132.